First Order Event Plane Correlated Directed and Triangular Flow in Au+Au Collisions from BES-II at STAR

Xiaoyu Liu[1,*] for the STAR Collaboration

[1]Department of Physics, The Ohio State University, 191 W Woodruff Ave, Columbus, OH 43210

Abstract. In heavy-ion collisions, the measurements of anisotropic flow coefficients (v_n) offer insights into collective hydrodynamic expansion and transport properties of the produced medium at higher collision energies, while also being sensitive to the compressibility of the nuclear matter and nuclear equation of state at lower collision energies. In this contribution, we present the measurement of charged particle v_1 over ten units of pseudorapidity (η) in Au+Au collisions at $\sqrt{s_{NN}}$=27 and 19.6 GeV and compare it with multiple model calculations. Only UrQMD was able to reproduce a sizable v_1 at the forward pseudorapidity as observed in the experiment. We also present the results of v_1 and v_3 at $\sqrt{s_{NN}}$=3-3.9 GeV for identified hadrons and light nuclei with respect to Ψ_1. The results are compared with theoretical models to identify the source of nonzero $v_3\{\Psi_1\}$ and to demonstrate its vital connection to the equation of state.

1 Introduction

Anisotropic flow measures the momentum-space correlation of the final state particles in the heavy-ion collisions. It can be characterized by the coefficients in the Fourier expansion of the azimuthal particle distribution with respect to the symmetry planes called event planes.The first order flow (v_1) coefficient, also referred to as directed flow, describes the collective sideward motion of the produced particles and nuclear fragments in heavy-ion collisions. It probes the system at the earliest stage because the deflection takes place during the passing time of the colliding nuclei. Model studies have indicated that directed flow is sensitive to the shear viscosity of the hot QCD matter [1]. Furthermore, directed flow has demonstrated strong constraining power on the initial baryon stopping and can serve as a probe for the equation of state in heavy-ion collisions [2].Therefore, the measurement of directed flow over a wide pseudorapidity range will offer valuable constraints on the three-dimensional initial state and evolution of the colliding system. In 2018, the Event Plane Detector (EPD, $2.1 < |\eta| < 5.1$) [3] was installed at STAR and was used for the Beam Energy Scan phase-II (BES-II) data taking. The combination of EPD and high-statistics BES-II data enables us to extend the directed flow measurement to the forward and backward pseudorapidity with high precision.

The third order flow (v_3), also referred to as triangular flow is usually attributed to the event-by-event fluctuations of the participant region geometry [4]. However, recent measurement has shown that there is a non-zero v_3 correlated with the first order event plane at lower collision energies [5]. The fixed-target program at STAR, covering collision energies from $\sqrt{s_{NN}}$ =3 to 7.7 GeV, provides an ideal test ground for studying this phenomenon.

*e-mail: liu.6566@osu.edu

2 Flow measurement at $\sqrt{s_{NN}}$ =19.6 and 27 GeV

In this analysis, the STAR Time Projection Chamber (TPC) ($|\eta| < 1.0$) was chosen as the reference to suppress the momentum conservation effect [6], while the EPD was used as the particles of interest region to extend the v_1 measurement to a wide pseudorapidity range. Figure 1 shows $v_1(\eta)$ measured at $\sqrt{s_{NN}}$ =19.6 and 27 GeV (integrated over the whole p_T space). At both energies, directed flow changes sign around the beam rapidity. Figure 2 shows the comparison with the PHOBOS measurement [7]. At all the energies, the $v_1(\eta - y_{\rm beam})$ curves fall on top of each other around $(\eta - y_{\rm beam}) \sim 0$. This scaling, usually referred to as the phenomenon of limiting fragmentation was first observed with $\frac{dN}{d\eta}$ [8]. It is interesting to see this phenomenon extend beyond yields to dynamics, as it might offer insights into the particle production mechanism in the fragmentation region. Figure 3 and Figure 4 shows various model comparisons. The UrQMD [9] $v_1(\eta)$ was calculated both with respect to the reaction plane and the event plane, the discrepancy between $v_1(\eta)\{\rm RP\}$ and $v_1(\eta)\{\rm EP\}$ can originate from several sources including the lumpiness of the colliding nuclei and the non-flow correlations. This UrQMD study underscores the importance of using the same reference when comparing the model calculations with the experimental measurements. The McGill hydrodynamic model [2] used at $\sqrt{s_{NN}}$ =19.6 GeV and the vHLLE hybrid model [10] used at $\sqrt{s_{NN}}$ =27 GeV are all one-fluid models. All of them produced very small v_1 at large pseudorapidity, while UrQMD was able to reproduce a sizable v_1 at the forward region as observed in the experiment. This comparison demonstrates the importance of incorporating all segments of the heavy-ion collision in model studies, especially at BES energies where nuclear fragments can substantially influence particle production across the entire pseudorapidity range.

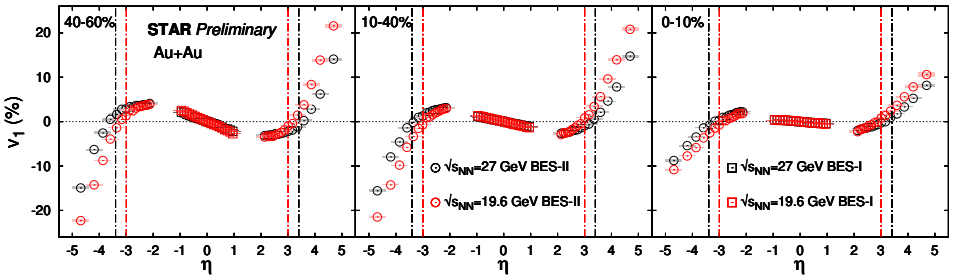

Figure 1. $v_1(\eta)$ measured across ten units of pseudorapidity for three centralities at $\sqrt{s_{NN}}$ =19.6 and 27 GeV. Black dashed lines represent the beam rapidity ($y_{\rm beam}$ = 3.4) at $\sqrt{s_{NN}}$ =27 GeV, red dashed lines represent the beam rapidity ($y_{\rm beam}$ = 3.0) at $\sqrt{s_{NN}}$ =19.6 GeV. The data points around the midrapidity are from the BES-I measurement where a p_T cut was applied [11].

3 Flow measurement at fix-target energies

In the STAR fixed-target mode, one of the RHIC beams is directed to collide with a fixed-target holder located just outside the TPC. Figure 5 shows the $v_3\{\Psi_1\}$ of protons measured in $0 < y < 0.5$ at $\sqrt{s_{NN}}$ =3 GeV [12]. It is negative at positive rapidity, which is opposite to the previously measured $v_1\{\Psi_1\}$ at the same energy [13]. Figure 6 shows the proton density distribution in $0.6 < y < 0.85$ sampled from JAM [14] at $\sqrt{s_{NN}}$ =3 GeV. The black arrows represent $\langle p_T \rangle$ in each cell, suggesting a positive v_1 at this rapidity slice. While the particle distributions is mainly dominated by the first-order flow component, the third-order

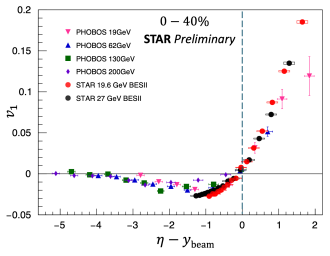

Figure 2. $v_1(\eta - y_{\rm beam})$ at various energies measured by the STAR and PHOBOS experiments.

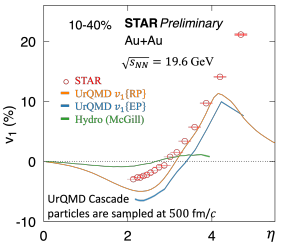

Figure 3. Model comparison at $\sqrt{s_{NN}}$ =19.6 GeV

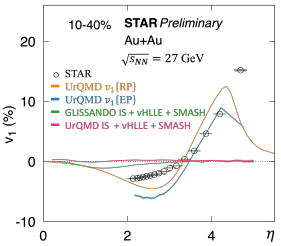

Figure 4. Model comparison at $\sqrt{s_{NN}}$ =27 GeV

flow component can be inferred from the geometry of the proton density distribution. The red arrows represent the direction of the pressure gradient, along which more particles are emitted, resulting in a negative $v_3\{\Psi_1\}$. Furthermore, the magnitude of $v_3\{\Psi_1\}$ is found to increase towards the peripheral collisions, indicating the collision geometry drives $v_3\{\Psi_1\}$ at this collision energy. Figure 5 also depicts the JAM calculation in the cascade mode (black dashed line) and with a relativistic mean field potential (red dashed line, K=380 MeV). It demonstrates that the nuclear potential is essential for the development of $v_3\{\Psi_1\}$. Figure 7 shows $v_3\{\Psi_1\}$ of proton measured at three more energies. Non-zero $v_3\{\Psi_1\}$ was observed from $\sqrt{s_{NN}}$ =3 to 3.9 GeV and JAM with a nuclear potential was able to reproduce the centrality and energy dependence of the measured $v_3\{\Psi_1\}$.

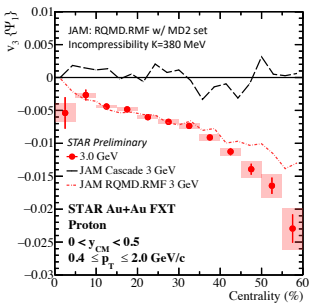

Figure 5. $v_3\{\Psi_1\}$ of protons as a function of centrality measured at $\sqrt{s_{NN}}$ =3 GeV. The red dashed line is the JAM calculation with a mean field potential, the black dashed line is the JAM calculation in the cascade mode.

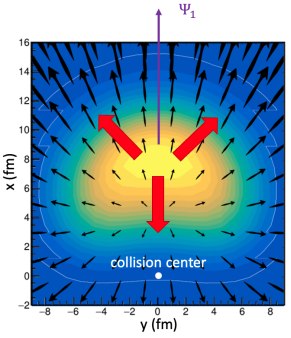

Figure 6. Proton density distribution from JAM sampled at 50 fm/c at $\sqrt{s_{NN}}$ =3 GeV for $0.6 < y < 0.85$. Black arrows represent $\langle p_T \rangle$ in each cell, red arrows represent pressure gradient.

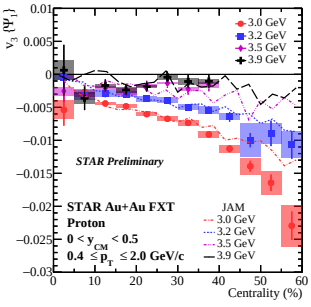

Figure 7. $v_3\{\Psi_1\}$ of protons as a function of centrality measured at four fix-target energies, the model calculations (dashed lines) are done by JAM with a mean field potential.

Besides proton, the $v_3\{\Psi_1\}$ and $v_1\{\Psi_1\}$ of deuteron, triton, Helium-3 and Helium-4 were also measured at $\sqrt{s_{NN}}$ =3 GeV and are shown in Figure 8 and 9. The atomic number scaling of $v_3\{\Psi_1\}$ and $v_1\{\Psi_1\}$ holds at $y < 0.5$, indicating the production of light nuclei comes from coalescence. However, this atomic number scaling breaks at $y > 0.5$.

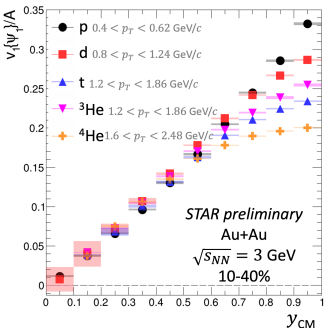

Figure 8. $v_1\{\Psi_1\}$ of light nuclei scaled by the atomic number as a function of rapidity

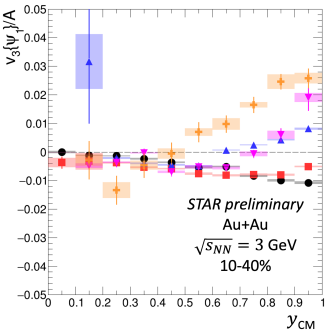

Figure 9. $v_3\{\Psi_1\}$ of light nuclei scaled by the atomic number as a function of rapidity. The legend is the same as that used in Figure 8

4 Summary

Directed flow was measured over a wide pseudorapidity at $\sqrt{s_{NN}}$ =19.6 and 27 GeV. "Limiting fragmentation" of v_1 was observed at all the centralities. Model comparison suggests nuclei fragments contribute substaintially to v_1 at large $|\eta|$. At fix-target energies, significant proton $v_3\{\Psi_1\}$ that has opposite sign from $v_1\{\Psi_1\}$ has been measured. The centrality dependence together with model calculations show $v_3\{\Psi_1\}$ is driven by the collision geometry. Model studies also suggests the nuclear potential is crucial for the development of $v_3\{\Psi_1\}$. Light nuclei v_1 and $v_3\{\Psi_1\}$ were also measured at $\sqrt{s_{NN}}$ =3 GeV. The observed atomic number scaling at $y < 0.5$ suggests the light nuclei are likely produced by the coalescence mechanism.

References

[1] F. Becattini, G. Inghirami, V. Rolando, A. Beraudo, L. Del Zanna, A. De Pace, M. Nardi, G. Pagliara, V. Chandra, Eur. Phys. J. C **75**, 406 (2015), [Erratum: Eur.Phys.J.C 78, 354 (2018)], 1501.04468

[2] L. Du, C. Shen, S. Jeon, C. Gale, Phys. Rev. C **108**, L041901 (2023), 2211.16408

[3] J. Adams et al., Nucl. Instrum. Meth. A **968**, 163970 (2020), 1912.05243

[4] B. Alver, G. Roland, Phys. Rev. C **81**, 054905 (2010), [Erratum: Phys.Rev.C 82, 039903 (2010)], 1003.0194

[5] J. Adamczewski-Musch et al. (HADES), Phys. Rev. Lett. **125**, 262301 (2020), 2005.12217

[6] N. Borghini, P.M. Dinh, J.Y. Ollitrault, A.M. Poskanzer, S.A. Voloshin, Phys. Rev. C **66**, 014901 (2002), nucl-th/0202013

[7] B.B. Back et al. (PHOBOS), Phys. Rev. Lett. **97**, 012301 (2006), nucl-ex/0511045

[8] B. Alver et al. (PHOBOS), Phys. Rev. C **83**, 024913 (2011), 1011.1940

[9] S.A. Bass et al., Prog. Part. Nucl. Phys. **41**, 255 (1998), nucl-th/9803035

[10] I. Karpenko, P. Huovinen, M. Bleicher, Comput. Phys. Commun. **185**, 3016 (2014), 1312.4160

[11] J. Adam et al. (STAR), Phys. Rev. C **101**, 024905 (2020), 1908.03585

[12] (2023), 2309.12610

[13] M.S. Abdallah et al. (STAR), Phys. Lett. B **827**, 137003 (2022), 2108.00908

[14] Y. Nara, H. Stoecker, Phys. Rev. C **100**, 054902 (2019), 1906.03537